Journal of Alloys and Compounds 509 (2011) 7525–7528

Contents lists available at ScienceDirect

Journal of Alloys and Compounds

journal homepage: www.elsevier.com/locate/jallcom

Preparation of $Sr_2Si_5N_8:Eu^{2+}$ for white light-emitting diodes by multi-step heat treatment

Van Duong Luong, Wentao Zhang, Hong-Ro Lee*

Department of Applied Materials Engineering, Chungnam National University, Daejeon 305-764, Republic of Korea

ARTICLE INFO

Article history:
Received 11 January 2011
Received in revised form 20 April 2011
Accepted 20 April 2011
Available online 28 April 2011

Keywords:
Red-emitting phosphor
White LEDs
Nitride phosphor
$Sr_2Si_5N_8$ synthesis
Multi-step heat treatment

ABSTRACT

In order to enhance luminescence properties of Eu^{2+}-doped ternary nitride phosphor for white light-emitting diodes (LEDs), $Sr_2Si_5N_8:Eu^{2+}$ phosphors with different Eu^{2+} concentrations were synthesized using a multi-step heat treatment. Impurities and luminescence properties of prepared $Sr_2Si_5N_8:Eu^{2+}$ phosphors were investigated using X-ray diffraction (XRD) and photoluminescence spectroscopy. Excitation spectra of $Sr_2Si_5N_8:Eu^{2+}$ phosphor showed broad excitation bands by both UV and blue light. Emission peak positions in spectra were red-shifted from 613 to 671 nm as Eu^{2+} ion concentrations increased. Phosphors following a multi-step heat treatment showed excellent luminescence properties. These included high emission intensity and very low thermal quenching compared to measurements using a commercially available YAG:Ce^{3+} phosphor.

1. Introduction

Low cost, easily fabricated white light emitting diodes (LEDs) with a high degree of brightness have drawn much attention since the finding that cool white light emission could be generated by combining the blue emission of InGaN diode chip with the yellow luminescence from $Y_3Al_5O_{12}:Ce^{3+}$ (YAG:Ce^{3+}) phosphor [1–4]. However, this white light has a low color rendering index (CRI) because the emitted yellow light lacks sufficient red emission. In order to obtain a good color rendering, warm white light output within a phosphor can be generated by two methods. One is to compensate the red deficiency of YAG:Ce^{3+}-based LED with a separate red light [5], and the other is to combine an UV chip with red, green, and blue-emitting (RGB) phosphors [6]. For both methods red phosphors that can be efficiently excited by InGaN LED chip are in great demand.

In recent years, SiN_4-base covalent nitride materials, including nitridosilicates, nitridoaluminosilicates and other nitrides, etc., have been extensively studied as good host lattices for LEDs, such as $M_2Si_5N_8:Eu^{2+}$ and $MAlSiN_3:Eu^{2+}$ (M = Ca, Sr, Ba) [7–16]. Among these phosphors, $Sr_2Si_5N_8:Eu^{2+}$ has demonstrated high luminescence intensity and very low thermal quenching. Several approaches have been tried for synthesizing $Sr_2Si_5N_8:Eu^{2+}$ phosphor, including a traditional solid-state reaction method using nitride raw materials and a reaction between metals and silicon diimide $Si(NH)_2$ [10,17]. These materials are not only expensive but also very sensitive to oxygen and moisture, thus $Si(NH)_2$ is difficult to prepare with pure grade reagents. The carbothermal reduction and nitridation (CRN) method can significantly decrease optical properties of phosphors, because the obtained phosphors can be easily contaminated by residual carbon [7,9]. Although acetate is used as a reducing agent for reduction and nitridation [16], acetate decomposes at low temperatures, which cannot ensure the complete reduction of oxides. Xie et al. [18] reported a synthetic route to $Sr_2Si_5N_8:Eu^{2+}$ phosphor using $SrCO_3$, Eu_2O_3, and Si_3N_4 as raw materials. However, the resultant product was a complex mixture of $Sr_2Si_5N_8$, α-Sr_2SiO_4 and β-Sr_2SiO_4. Therefore, an efficient method is needed to synthesize the red $Sr_2Si_5N_8:Eu^{2+}$ phosphor with pure-phase and enhanced luminescence properties.

We used a multi-step heating approach to synthesize $Sr_2Si_5N_8:Eu^{2+}$ phosphor. All the raw materials used were commercially available, used low cost oxides, and the synthesis can be accomplished in an ambient atmosphere. The effect of Eu^{2+} ion concentration on the luminescence properties of the prepared phosphors was evaluated. Additionally, the structure and the luminescence properties of the synthesized $Si_2Si_5N_8:Eu^{2+}$ phosphor were investigated and compared with the commercially available YAG:Ce^{3+} phosphor.

2. Experimental

2.1. Preparation of $(Sr_{1-x}Eu_x)_2Si_5N_8$ (x = 0–0.2)

All powder samples of $(Sr_{1-x}Eu_x)_2Si_5N_8$ were synthesized using a multi-step heating method from the raw materials of strontium carbonate ($SrCO_3$, 99.9%),

* Corresponding author. Tel.: +82 42 821 5638; fax: +82 42 825 5638.
E-mail address: leehr@cnu.ac.kr (H.-R. Lee).

0925-8388/$ – see front matter © 2011 Elsevier B.V. All rights reserved.
doi:10.1016/j.jallcom.2011.04.109

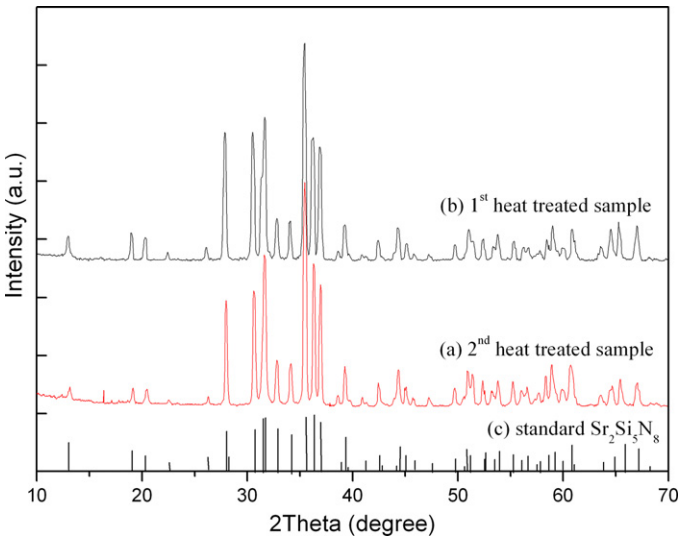

Fig. 1. XRD patterns of the 2nd heat treated specimen (a) vs. standard specimen of $Sr_2Si_5N_8$:Eu^{2+} (b).

silicon nitride (Si_3N_4, 99.5%), europium oxide (Eu_2O_3, 99.99%), and activated charcoal powder (C, 99.99%). The concentration of Eu^{2+} varied in a range of 0–20 at.% with respect to Sr^{2+}. They were stoichiometrically weighed and mixed thoroughly in an agate mortar. Mixtures were pressed into a graphite crucible placed into an induction furnace. The furnace chamber was evacuated and filled with pure N_2, and a flow rate of 1000 mL/min was maintained during the heating process. For the first heat step the temperature was rapidly raised to 1100 °C and maintained for 1 h to decompose $SrCO_3$ completely. Next the temperature was increased to 1400 °C and maintained for 3 h to form $(Sr_{1-x}Eu_x)_2Si_5N_8$ phosphor (1st heat treated specimen). Finally, the 1st heat treated specimens were transferred into a molybdenum crucible, and sintered again at 1600 °C under N_2 gas flow for 3 h. After firing, the obtained phosphors (2nd heat treated specimen) were cooled in a furnace under a continuous flow of N_2 gas.

2.2. Characterization

The crystalline phase of the synthesized $Sr_2Si_5N_8$:Eu^{2+} powder was measured using X-ray powder diffraction (SIEMENS X-ray diffractometer) with Cu Kα radiation (λ = 1.5406 Å). The data were collected in the 2θ range from 10° to 70° with a scanning rate of 3°/min. Diffuse reflection spectra were obtained using a $BaSO_4$ powder calibrated UV–vis spectrophotometer (UV-2200, SHIMADZU). Photoluminescence (PL) measurement was carried out at room temperature using 455 nm as the excitation wavelength with a Perkin Elmer LS-45 luminescence spectrometer. The temperature dependence of photoluminescence was measured with a multichannel spectrophotometer (model MCPD7000; Otsuka Electronics) equipped with temperature-controlled sample holders and a Xe lamp. Oxygen, nitrogen, and carbon content of obtained phosphors were measured using an oxygen/nitrogen analyzer and carbon analyzer and were compared to chemically analyzed values.

3. Results and discussion

3.1. Structure and phase purity

The crystal structures of synthesized $Sr_2Si_5N_8$:Eu^{2+} phosphors showed an orthorhombic lattice with the space group of $Pmn2_1$ [17]. Fig. 1 gives the X-ray diffraction (XRD) pattern of the 2nd heat treated specimen compared by standard specimen. Most of the diffraction peaks of synthesized $Sr_2Si_5N_8$:Eu^{2+} phosphors showed identical peaks to the standard specimen and no apparent impurity phases were found. Moreover, it was also indexed that the

Table 1
Oxygen, nitrogen, and carbon contents (wt%) of $Sr_2Si_5N_8$:Eu^{2+} (2 at.%) phosphors.

$Sr_2Si_5N_8$:Eu^{2+}	O	N	C
1st heat treated sample	1.70	25.10	0.26
2nd heat treated sample	0.82	25.90	0.04
Ideal	0	26.20	0

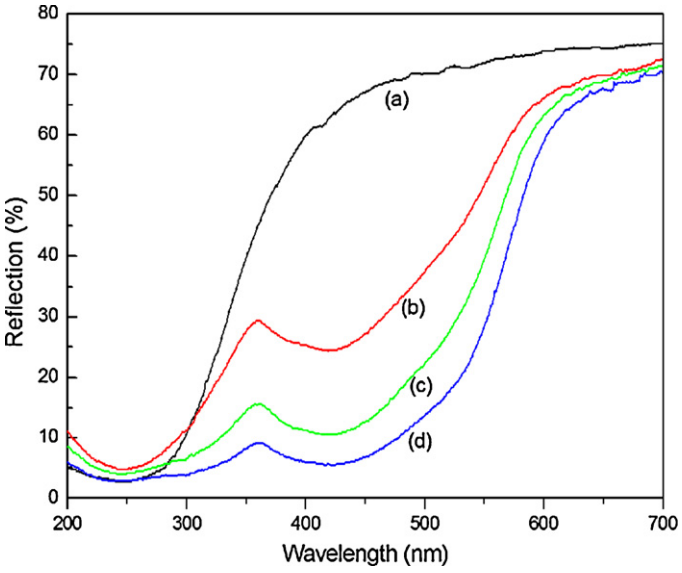

Fig. 2. Diffuse reflection spectra of undoped $Sr_2Si_5N_8$ host (a) and $(Sr_{1-x}Eu_x)_2Si_5N_8$ phosphor with x 0.02 (b), 0.1 (c), and 0.2 (d).

doped Eu^{2+} ions did not caused any significant change in the host structure.

Carbon powder was used as raw material to synthesize $Sr_2Si_5N_8$:Eu^{2+} phosphor, so the oxygen, nitrogen and residual carbon contents always exist in the prepared $Sr_2Si_5N_8$:Eu^{2+} phosphor. These elemental contents (O, N, and C) were measured using an O/N analyzer and a carbon analyzer. After the 1st heat treated specimens were sintered again at 1600 °C, carbon and oxygen were removed as CO by a bonding effect, so small amount of oxygen (about 0.82 wt%) and carbon (about 0.04 wt%) were detected (Table 1).

3.2. Photoluminescence properties

The optical reflection spectra of $Sr_2Si_5N_8$:Eu^{2+} phosphors with different Eu^{2+} ion concentration are shown in Fig. 2. For all samples, two strong absorption bands were presented in the range of the UV to visible spectra region, the first absorption band at 250–350 nm was caused by the electronic transition of the $Sr_2Si_5N_8$ host and

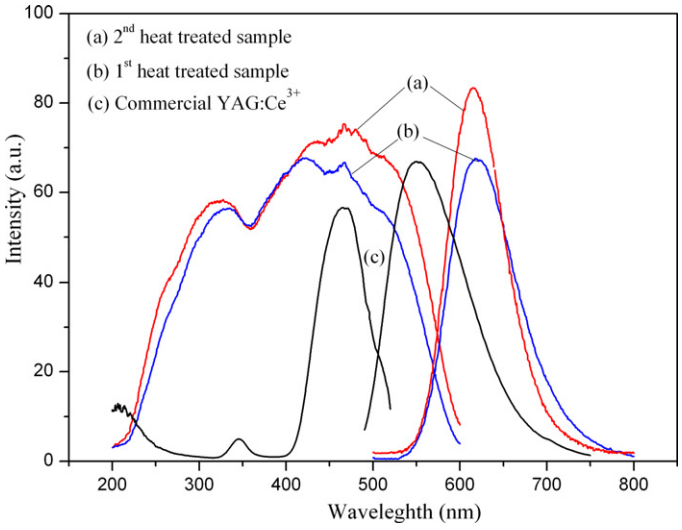

Fig. 3. Typical photoluminescence spectra of the $Sr_2Si_5N_8$:Eu^{2+} (2 at.%) phosphor with the 2nd heat treated specimen (a), 1st heat treated specimen (b) and commercial YAG:Ce^{3+} phosphor (c).

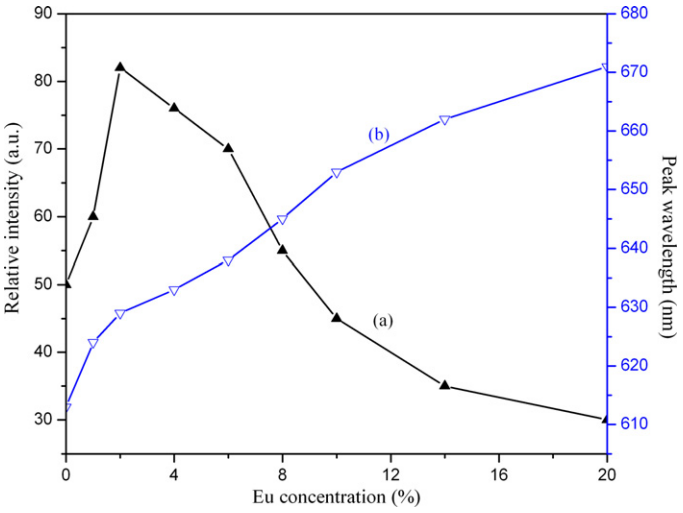

Fig. 4. Dependence of emission intensity (a) and peak emission wavelength (b) as a function of Eu concentration in $(Sr_{1-x}Eu_x)_2Si_5N_8$ phosphor under 455 nm excitation.

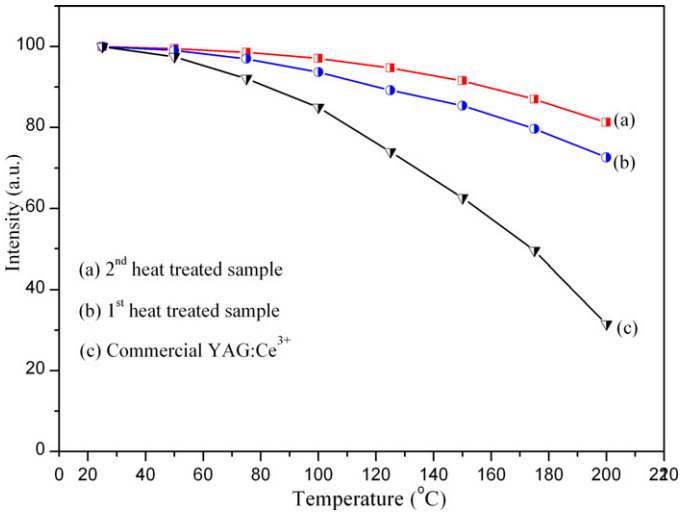

Fig. 6. Temperature quenching of the $Sr_2Si_5N_8:Eu^{2+}$ (2 at.%) phosphors of the 2nd heat treated specimen (a), the 1st heat treated specimen (b) and commercial YAG:Ce^{3+} phosphor (c).

the second absorption band at 350–550 nm can be assigned to the $4f^7 \rightarrow 4f^65d^1$ transition of Eu^{2+} ion. The absorption becomes stronger and the absorption edges shift to the longer wavelength with increasing Eu^{2+} concentration so that the body color of phosphors reddens gradually.

Photoluminescence (excitation/emission) spectra of the $Sr_2Si_5N_8:Eu^{2+}$ (2 at.%) phosphor, together with that of standard YAG:Ce^{3+} (P46-Y3) for comparison are plotted in Fig. 3. Excitation spectra consist of a broadband covering wave lengths from the UV to visible region. The broad band emission peak at 628 nm of the $Sr_2Si_5N_8:Eu^{2+}$ (2 at.%) phosphor at the excitation of 455 nm is assigned to the allowed $4f^65d^1 \rightarrow 4f^7$ transition of Eu^{2+} ion [15]. Due to the high covalent environment around Eu^{2+} ion, emission of $Sr_2Si_5N_8:Eu^{2+}$ phosphor was observed at a fairly longer wavelength region compared to $MF_2:Eu^{2+}$ or $M_2SiO_4:Eu^{2+}$ (M = Sr/Ba) [19,20]. In the present study, the 2nd heat treated specimens contained lower impurities such as residual carbon and oxygen (Table 1). Therefore luminescence intensity values showed a fairly enhanced result (Fig. 3). Calculated emission intensity was about 117% of YAG:Ce^{3+} at the same excitation of 455 nm.

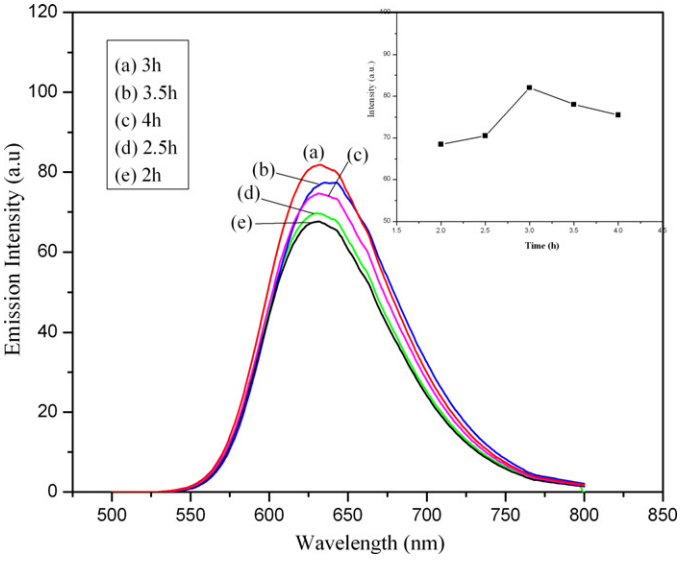

Fig. 5. Emission intensity of $Sr_2Si_5N_8:Eu^{2+}$ (2 at.%) according to heat treatment duration time.

Dependence of emission intensity and peak emission wavelength on Eu^{2+} concentration of the $(Sr_{1-x}Eu_x)_2Si_5N_8$ phosphor is shown in Fig. 4. With increasing Eu^{2+} content, emission intensity of $(Sr_{1-x}Eu_x)_2Si_5N_8$ phosphor was maximized at a Eu^{2+} concentration around 2 at.% (i.e., $x = 0.02$) and then decreased slowly with doping of more Eu^{2+}. The decrease in emission intensity beyond a critical concentration is ascribed to the concentration quenching which is mainly caused by the energy transfer between two Eu^{2+} ions. Because both excitation and emission bands due to $4f^65d$–$4f^7$ transition of Eu^{2+} ion are allowed as well as their overlap in the 550–610 nm range of wavelengths, the energy transfer may occur as a result of multipolar interaction and radiation reabsorption. Meanwhile, the peak emission of $(Sr_{1-x}Eu_x)_2Si_5N_8$ phosphor shifted to the longer wavelength side (red shift) as Eu^{2+} concentration increased from 0 to 20 at.%.

Emission intensity of $Sr_2Si_5N_8:Eu^{2+}$ (2 at.%) corresponding to heat treatment duration time is shown in Fig. 5. The highest emission intensity was observed at the 3 h heat treatment duration time. This result may be caused by a decrease in impurities as holding time increased due to the reaction of carbon with oxygen to more thoroughly produce carbon monoxide, which increased emission intensity. However when holding time was increased beyond the 3 h treatment, emission intensity showed an obvious decrease.

Phosphors for white LEDs should have low thermal quenching to avoid changes in chromaticity and brightness of white LEDs at high temperatures. The temperature-dependent emission intensity of $Sr_2Si_5N_8:Eu^{2+}$ (2 at.%) phosphors and YAG:Ce^{3+} phosphors are shown in Fig. 6. As the temperature increased from 20 to 200 °C, the emission peak of $(Sr_{0.98}Eu_{0.02})_2Si_5N_8$ phosphor was kept at the 628 nm position, but the intensity was decreased by 18% of the initial value, whereas the decrease for the YAG:Ce^{3+} phosphor was 64%. This result may be due to improved activity of oxygen within the phosphors as temperature increased. As the energy transferred to nonradiative emission increased temperature-dependent emission the intensity correspondingly decreased. As oxygen content was increased a greater decrease in intensity was observed.

4. Conclusions

$Sr_2Si_5N_8:Eu^{2+}$ red phosphor has been successfully synthesized using a multi-step heating method. The 2nd heat treated specimens have a single-phase crystalline structure of $Sr_2Si_5N_8$ and showed

very low carbon and oxygen impurities. Synthesized phosphors doped with Eu^{2+} ions up to 2 at.% were efficiently excited by the blue light (455 nm) and showed a red emission peak at 628 nm. After the 2nd heat-treatment, luminescence properties of obtained $Sr_2Si_5N_8:Eu^{2+}$ phosphors were obviously enhanced compared with those of commercially available YAG:Ce^{3+} phosphors.

References

[1] N. Jia, X. Zhang, W. He, W. Hu, X. Meng, Y. Du, J. Jiang, Y. Du, J. Alloys Compd. 509 (2011) 1848–1853.
[2] J.R. Oh, S.H. Cho, Y.H. Lee, Y.R. Do, Opt. Express 17 (2009) 7450–7457.
[3] C.W. Won, H.H. Nersisyan, H.I. Won, J.H. Lee, K.H. Lee, J. Alloys Compd. 509 (2011) 2621–2626.
[4] V. Bachmann, C. Ronda, A. Meijerink, Chem. Mater. 21 (2009) 2077–2084.
[5] Q. Shao, H. Li, Y. Dong, J. Jiang, C. Liang, J. He, J. Alloys Compd. 498 (2010) 199–202.
[6] J.K. Sheu, S.J. Chang, C.H. Kuo, Y.K. Su, L.W. Wu, Y.C. Lin, W.C. Lai, J.M. Tsai, G.C. Chi, R.K. Wu, IEEE Photon. Technol. Lett. 15 (2003) 18–20.
[7] X. Piao, T. Horikawa, H. Hanzawa, K. Machida, Appl. Phys. Lett. 88 (2006) 161908.
[8] M. Zeuner, F. Hintze, W. Schnick, Chem. Mater. 21 (2009) 336–342.
[9] B. Lee, S. Lee, H.G. Jeong, K.-S. Sohn, ACS Comb. Sci. 13 (2011) 154–158.
[10] H.A. Höppe, H. Lutz, P. Morys, W. Schnick, A. Seilmeier, J. Phys. Chem. Solids 61 (2000) 2001–2006.
[11] X. Teng, C. Liang, J. He, J. Semicond. 32 (2011) 012003.
[12] Y.Q. Li, G. de With, H.T. Hintzen, J. Solid State Chem. 181 (2008) 515–524.
[13] H. Watanab, N. Kijima, J. Alloys Compd. 475 (2009) 434–439.
[14] K.-S. Sohn, S. Lee, R.-J. Xie, N. Hirosaki, Appl. Phys. Lett. 95 (2009) 161908.
[15] Y. Zhou, Y. Yoshizawa, K. Hirao, Z. Lenčéš, P. Šajgalík, J. Eur. Ceram. Soc. 31 (2011) 151–157.
[16] X. Piao, K. Machida, T. Horikawa, B. Yun, J. Lumin. 130 (2010) 8–12.
[17] Y.Q. Li, A.C.A. Delsing, R. Metslaar, G. de With, H.T. Hintzen, J. Alloys Compd. 487 (2009) 28–33.
[18] R.J. Xie, N. Hirosaki, T. Suehiro, F.F. Xu, M. Mitomo, Chem. Mater. 18 (2006) 5578–5583.
[19] D.B. Gatch, D.M. Boye, Y.R. Shen, M. Grinberg, Y.M. Yen, R.S. Meltzer, Phys. Rev. B 74 (2006) 195117.
[20] J.K. Park, K.J. Choi, C.H. Kim, H.D. Choi, S.Y. Park, Electrochem. Solid-State Lett. 7 (2004) H15–H17.